Neurochemistry International 186 (2025) 105973

Contents lists available at ScienceDirect

Neurochemistry International

journal homepage: www.elsevier.com/locate/neuint

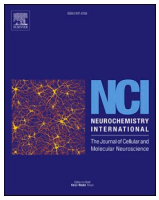

Sp4/HD11 and Sp1/HAT-p300 complexes induce apoptotic cell death in $CuCl_2$-treated neurons by modulating histone acetylation on BCL-W and BAX promoters

Silvia Ruggiero [a], Natascia Guida [a], Luigi Mascolo [a], Angelo Serani [b], Anna Ferrante [a], Francesca Galasso [a], Luca Sanguigno [a], Erica Piemonte [c,d], Elvira De Rosa [e], Paolo Montuori [f], Maria Triassi [f], Gianfranco Di Renzo [a], Mario Galgani [c,d], Luigi Formisano [a,*]

[a] Division of Pharmacology, Department of Neuroscience, Reproductive and Dentistry Sciences, School of Medicine, Federico II University of Naples, Via Pansini, 5, 8013, Naples, Italy
[b] Department of Neuroscience and Brain Technologies, Istituto Italiano di Tecnologia, Via Morego, 30, 16163, Genova, Italy
[c] Department of Molecular Medicine and Medical Biotechnology, Federico II University of Naples, Via Pansini, 5, 8013, Naples, Italy
[d] Laboratorio di Immunologia, Istituto per l'Endocrinologia e l'Oncologia Sperimentale "G. Salvatore, " Consiglio Nazionale delle Ricerche, Naples, Italy
[e] Department of Human Sciences and Quality of Life Promotion, San Raffaele University, 00166, Rome, Italy
[f] Department of Public Health, "Federico II" University, Via Sergio Pansini no 5, 80131, Naples, Italy

ARTICLE INFO

Keywords:
Copper
Neurotoxicity
Apoptosis
Cortical neurons
Histone acetylation

ABSTRACT

Copper is a metal physiologically present in the brain that becomes neurotoxic at high concentrations; on the other hand, pharmacological inhibition of Histone Deacetylases (HDs) or of Histone Acetyltransferases (HATs) reduce neuronal death caused by several neurotoxicants. Herein, we found that $CuCl_2$ (300 μM in SH-SY5Y cells or 100 μM in cortical neurons) determined apoptotic cell death, that was counteracted by the class IV HDs inhibitor Mocetinostat (MOCE) and by the HAT-p300 inhibitor C646, but not by the class I and II HDs inhibitors. Interestingly, HD11 and HAT-p300 protein levels increased after both 12 and 24 h of $CuCl_2$ exposure and their silencing partially limited $CuCl_2$-neurodetrimental effect. Furthermore, in $CuCl_2$-treated cells the transcriptional factor Sp4 co-localized with HD11 on the promoter of anti-apoptotic gene BCL-W, determining histone H3 hypo-acetylation, a marker of gene repression. Contrarily, Sp1 co-localized with HAT-p300 on the pro-apoptotic gene BAX, determining histone H4 hyper-acetylation, a hallmark of transcriptional activation. In addition, siRNA against Sp4 prevented HD11 binding on BCL-W promoter and its consequent down-regulation, whereas Sp1 knocking-down, by reducing HAT-p300 interaction on BAX gene promoter counteracted its up-regulation. Importantly, while the single knocking-down of Sp1, Sp4, HD11 and HAT-p300 partially mitigated $CuCl_2$-induced cell death, the double-transfection of siRNAs for Sp1 and Sp4, or for HD11 and HAT-p300, completely reverted the neurotoxic effect of $CuCl_2$. Collectively, we found that $CuCl_2$-induced neuronal apoptosis is determined by the binding of Sp1/HAT-p300 and of Sp4/HD11 transcriptional complexes on the BAX and BCL-W gene, respectively, unraveling a new pathway involved in Copper-induced neurotoxicity.

1. Introduction

Copper (Cu^{2+}) plays an indispensable role in the physiology of the human Central Nervous System (CNS); it's a cofactor of several enzymes and it contributes to the neurotransmitter biosynthesis, protection against reactive oxygen species (ROS), cellular respiration, pigment formation (Gaetke et al., 2014). As a consequence of its redox activity, copper cellular uptake, storage and export must be tightly regulated in order to prevent its overload (Zhong et al., 2024). Copper is also present as an environmental pollutant, originating from both natural and anthropogenic sources, and has a significant impact on human health (Rehman et al., 2019). Moreover, copper is naturally present in foods such as animal liver, nuts, legumes, fish, shrimp, and shellfish, whereas dairy products contain low levels (Kolbaum et al., 2023). The total copper content in the brain ranges from 3.1 μg/g to 5.1 μg/g (Joshi et al., 2021), and the risk of peripheral neuropathy starts to increase when the

* Corresponding author.
E-mail address: luigi.formisano@unina.it (L. Formisano).

https://doi.org/10.1016/j.neuint.2025.105973
Received 7 February 2025; Received in revised form 21 March 2025; Accepted 31 March 2025
Available online 2 April 2025

dietary copper intake reaches or exceeds 0.889 mg/d (Wu et al., 2024). Importantly, copper supplementation in the dietary is controversial: indeed, it is relevant in patients with an acquired copper deficiency, i.e. Menkes Syndrome (Tümer and Møller, 2010), whereas its overload in the CNS can be neuro detrimental (Scheiber et al., 2014). Notably, low-copper diet could be a preventive strategy for Alzheimer's disease (AD) (Squitti et al., 2014); copper accumulates in the hippocampus, that is the main brain region involved in AD pathophysiology, leading to memory and learning impairments in an *in vivo* model of brain copper toxicosis (Pal et al., 2013). Furthermore, it has been found that the blood-free copper pool was significantly increased in AD patients (Squitti et al., 2005). At biochemical level, Amyloid precursor protein (APP), β-site APP cleaving enzyme 1 (BACE1), Amyloid β (Aβ), and Tubulin-Associated Unit (Tau) proteins have been found to interact with copper, thus contributing to dysregulate copper homeostasis in the brain (Zhong et al., 2024). In particular, copper: (1) interacts with Aβ and reduces the expression of low-density lipoprotein receptor-related protein-1 (LRP1), thus enhancing neuroinflammation and Aβ clearance disorder (Ejaz et al., 2020) and (2) promotes tau hyperphosphorylation and aggregation (Zubčić et al., 2020). In Amyotrophic Lateral Sclerosis (ALS) patients, there are high levels of copper ions in the motor cortex (Tokuda et al., 2009). Moreover, mutations in SOD1 protein, by affecting copper ions metal binding properties, significantly disturbs its native structure, which is closely related to the progression of ALS (Enge et al., 2018). Notably, also in the brain of Huntington's disease (HD) patients, there are elevated copper levels (Hands et al., 2010). It has been proposed that copper, by binding mutant huntingtin (mHTT), promotes HTT fibril formation and oligomerization (Hands et al., 2010). Among the cell death mechanisms induced by copper, apoptosis plays a pivotal role. Indeed, Copper, by inducing the cleaved-caspase 3 activation (Kalita et al., 2017) and the release of cytochrome *c*, reduces cell survival in rat cortical neurons and neuronal-like PC12 cells (Sun et al., 2014), whereas in the hippocampus and frontal cortex of rat mimicking Wilson disease apoptosis is activated by glutamate release and oxidative stress pathways (Kalita et al., 2017). Furthermore, it has been reported that epigenetic modifications, such as histone protein acetylation and deacetylation, catalyzed by the Histone Acetylatransferase (HAT) and Histone deacetylases (HDs), respectively, are involved in the mechanisms by which neurotoxic agents, such as organic mercury, induce apoptotic neuronal death (Guida et al., 2015, 2016). HD enzymes are divided into four classes: the Class I (HD1-3 and HD8); the Class II (HD4-7, and HD9, 10); the Class III (SIRT1-7); and the Class IV (HD11) (Seto and Yoshida, 2014), whereas HATs are classified into: type A and type B. The interplay between HDs or HATs and the mechanisms leading to toxicity following Copper exposure is corroborated by several evidence. Indeed, it has been found that Copper at high or toxic levels: (1) decreases histone H4 acetylation levels in yeast cells (Broday et al., 2000), (2) increases the expression of HD4 and HD10 isoforms (Song et al., 2009) and inhibits HAT activity in hepatic cells (Kang et al., 2004). The recruitment of HDs and HATs by specific transcription factors (TFs) allow these chromatin-modifying enzymes to regulate specific genes. Among the TF, Sp1 and Sp3 proteins have been found to be modulated under Copper-stressed conditions, indeed their protein levels expression are influenced by Copper-replete or -depleted conditions in lung cancer cells (Liang et al., 2012). Furthermore, Sp1 is an essential transcription factor that serves as a Copper sensor, regulating Cu^{2+} homeostasis through the transcriptional control of key transporters and interactions with other regulatory proteins (Fitisemanu and Padilla-Benavides, 2024). There are four Sp isoforms: Sp1, Sp3 and Sp4 recognize the same Sp1 binding sequence with similar affinities (Formisano et al., 2015), whereas Sp2 does not bind to DNA or activate transcription when expressed in mammalian cell lines. Sp1, Sp3, and Sp4 can act as either activators or repressors of gene expression (Formisano et al., 2015). At pharmacological level, HDs inhibitors, that have been found neuroprotective against several neurotoxic agents, are classified in: (1) pan-HDs inhibitors, such as Trichostatin A (TSA) and Sodium Butyrate (NaBu), and (2) class-selective HDs inhibitors, such as MS-275, specific for HDs class I, MC-1568, specific for HDs class II and Mocetinostat, specific for HDs class I and IV (Huang et al., 2019). Accordingly, the pan-HDs inhibitor NaBu diminished Cu^{2+}-induced cytotoxicity by improving histone acetylation levels in leukemia cell line (Lin et al., 2005). On the other hand, HATs inhibitors can be divided into: (1) bi-substrate inhibitors, (2) natural products and (3) synthetic small molecules. Among these drugs, the synthetic small molecule C646 has been found able to reduce the amount of Tau and neurotoxicity in culture rat neurons (Min et al., 2010). Over the years, the role of Copper as an activator of apoptotic cell death has been investigated in several *in vitro* models, such as murine neocortical neurons (Sheline et al., 2002), cultured human neurons (Vanlandingham et al., 2005) and M17 human neuroblastoma cells (Chan et al., 2008). More specifically, it has been shown that mitochondria is a primary target of Copper-dependent toxicity (Arciello et al., 2005). Mitochondria-dependent apoptosis is regulated by the family of BCL-2 proteins, which finely balance the preservation or the disruption of mitochondrial cell membrane permeability. In particular, the anti-apoptotic members include: BCL-2, BCL-W (also known as BCL2-L2), BCL-xL, and MCL-1, whereas, the pro-apoptotic proteins are subdivided into: effector proteins (BAK and BAX) and BH3-only members (BAD, BID, BIK, BIM, BMF, bNIP3, HRK, Noxa, and PUMA) (Lomonosova and Chinnadurai, 2008). Regarding these anti- and pro-apoptotic proteins, it has been found that Copper-induced cell damage occurs via the reduction of BCL-2 and increase of BAX in hippocampal neurons (Lu et al., 2022a).

Since the correlation between histone acetylation and $CuCl_2$-induced apoptosis in neuronal cells has never been investigated, herein, we aimed to identify which epigenetic modifier of histone protein acetylation, among HDs and HATs, are specifically involved in Copper-induced neurotoxicity. Furthermore, we studied whether the transcription factors belonging to the Sp family are involved in this epigenetic mechanisms, by recruiting specific HD or HAT isoforms, and their role to modulate the pro-apoptotic gene BAX and anti-apoptotic gene BCL-2 in SH-SY5Y cells and cortical neurons exposed to $CuCl_2$.

2. Results

2.1. $CuCl_2$-induced apoptotic cell death was partially prevented by the class IV HD inhibitor Mocetinostat and HAT-p300 inhibitor C646 in SH-SY5Y cells

SH-SY5Y neuroblastoma cells exposed to $CuCl_2$ at 100–500 μM for 24 h showed a reduction in mitochondrial activity starting at 300 μM, as revealed by MTT analysis (Fig. 1A). Since 300 μM $CuCl_2$ damaged approximately 50 % of cells, this concentration was chosen for all experiments unless stated otherwise. To investigate the role of histone acetylation/deacetylation in modulating $CuCl_2$–induced neuronal death, cells were pre-treated with the inhibitors of: (1) class I HDs (MS-275) (Formisano et al., 2015; Laudati et al., 2019), class II HDs (MC-1568) (Guida et al., 2016; Laudati et al., 2019), class IV HDs (Huang et al., 2019) (Mocetinostat: MOCE), and (2) HAT (C646) (Formisano et al., 2015), at well-known neuroprotective concentrations. MTT and LDH assay experiments demonstrated that the survival of $CuCl_2$-treated cells significantly enhanced when cells were pre-treated with MOCE 70 nM and C646 20 μM (Fig. 1B and C). By contrast, any neuroprotective effects were observed after MS-275 and MC-1568 pre-treatments (Fig. 1B and C). In order to evaluate if the protective effect of MOCE and C646 on cell viability could be due to changes in apoptotic/dead cell numbers, we analyzed $CuCl_2$-treated cells by using the TaliTM Apoptosis assay kit-Annexin V Alexa Fluor® 488 and propidium iodide. Specifically, Fig. 1D shows the percentage of live, dead and apoptotic cells after each treatment. Notably, in $CuCl_2$-treated cells the percentage of apoptotic and dead cells was significantly higher compared to CTL group, furthermore, pre-treatment with MOCE and C646 was able to significantly reduce apoptotic and dead cells,

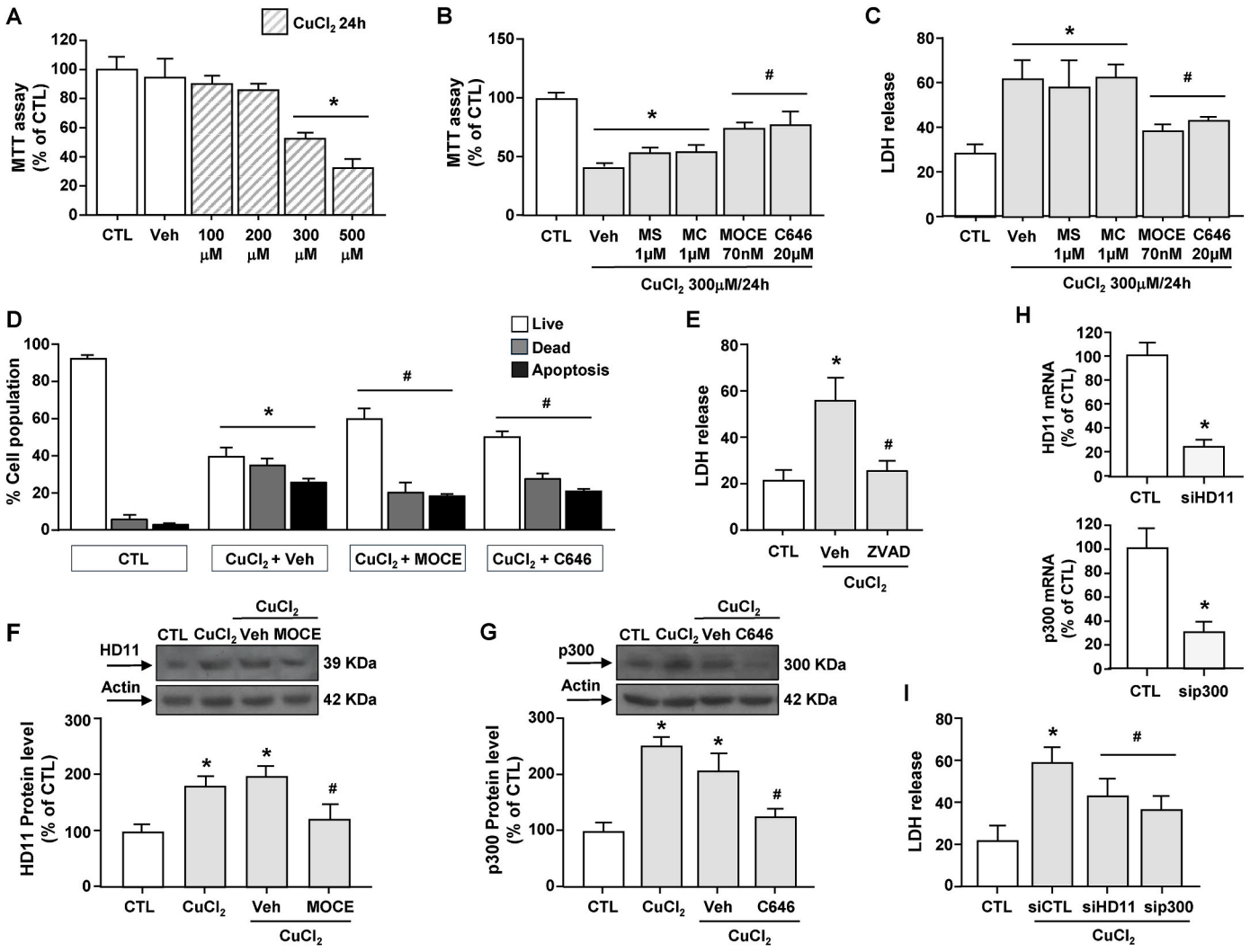

Fig. 1. Effect of $CuCl_2$, alone or in combination with HD or HAT inhibitors, on cell survival and on HD11 and HAT-p300 expression in SH-SY5Ycells. (**A**) Effects of 24 h exposure to $CuCl_2$ at 100, 200, 300, and 500 µM on cell death, as evaluated by MTTassay. Each bar represents mean ± SD obtained from 4 independent experimental sessions. *P < 0.05 vs CTL. (**B, C**) Effect of 300 µM $CuCl_2$ at 24 h, alone or with 1 µM of MS-275 (MS) or MC-1568 (MC), 70 nM Mocetinostat (MOCE) and 20 µM C646 on mitochondrial activity (**B**) and LDH release (**C**). Cells were pre-treated with epi-drugs for 2 h before $CuCl_2$ administration. Each bar represents mean ± SD obtained from 4 independent experimental sessions. *P < 0.05 vs CTL; #P < 0.05 vs $CuCl_2$+ Vehicle. (**D**) Effect of 24 h of $CuCl_2$ at 300 µM, alone or after 2 h of pretreatment with MOCE or C646 on propidium iodide (PI) (index of dead cells) and Annexin V staining (index of apoptotic cells). Percentage of live, dead and apoptotic cells after each treatment, determined by Tali® Image-Based cytometer. Each bar represents mean ± SD obtained from 3 independent experimental sessions. *P < 0.05 vs respective control group (CTL); #P < 0.05 vs $CuCl_2$+ Veh. (**E**) Effect of 24 h of $CuCl_2$ at 300 µM, alone or in combination with ZVAD (200 µM) on LDH release. Each bar represents mean ± SD obtained from 4 independent experimental sessions. *P < 0.05 vs vehicle; *P < 0.05 vs CTL; #P < 0.05 vs $CuCl_2$+ Veh. (**F, G**) Representative western blotting of HD11 (**F**) and HAT-p300 (**G**) in SH-SY5Y treated for 24 h with $CuCl_2$ (300 µM), alone or after 2 h of pre-treatment with MOCE (**F**) or C646 (**G**). Each bar represents mean ± SD obtained from 3 independent experimental sessions. *P < 0.05 vs CTL; #P < 0.05 vs $CuCl_2$. (**H**) RT-PCR for HD11 and p300, in cells transfected for 48 h with siCTL, siHD11, and sip300 at a final concentration of 50 nM. Each bar represents mean ± SD obtained from 3 independent experimental sessions. *P < 0.05 vs siCTL. (**I**) Effect of 24 h of $CuCl_2$ at 300 µM, alone or after transfection with siCTL, siHD11, and sip300 on LDH release. Each bar represents mean ± SD obtained from 4 independent experimental sessions. *P < 0.05 vs siCTL; #P < 0.05 vs $CuCl_2$.

compared to $CuCl_2$+Vehicle-treated cells (Fig. 1D). To further confirm the apoptotic nature of $CuCl_2$-induced cell death, LDH assay experiments demonstrated that $CuCl_2$-induced cell death was significantly prevented by apoptotic inhibitor ZVAD 200 µM (von Coelln et al., 2001) (Fig. 1E).

Next, since MOCE and C646 were the only drugs able to limit $CuCl_2$-induced cell death, we evaluated the protein expression of HDAC11 and HAT-p300, their respective targets, in $CuCl_2$-treated SH-SY5Y cells. As shown in Fig. 1F and G, MOCE and C646 reverted $CuCl_2$-induced HD11 and HAT-p300 protein levels increase. As expected, HD11 and HAT-p300 knocking-down by siRNAs transfection, that significantly reduced HD11 and HAT-p300 mRNA expression of almost 70 % (Fig. 1H), were both able to counteract $CuCl_2$-induced cell survival reduction (Fig. 1I). These results indicated that MOCE and C646, by blocking HD11 and HAT-p300 increase, respectively, limited $CuCl_2$-induced apoptotic neuronal death.

2.2. *Sp4/HD11 and Sp1/HAT-p300 complexes co-localized on BCL-W and BAX gene promoters, respectively, in $CuCl_2$-treated SH-SY5Y cells*

Since the epigenetic remodelers HDs and HATs are recruited to their target regions by sequence-specific regulatory proteins (e.g. transcription factors: TFs) and the TF Sp1 is known to regulate Copper homeostasis (Song et al., 2008), we investigated in $CuCl_2$-treated cells whether Sp family members might interact with HD11 and HAT-p300. Notably, among Sp isoforms, only Sp1 (Fig. 2A) and Sp4 (Fig. 2C), but not Sp3 (Fig. 2B), resulted significantly up-regulated after 24 h $CuCl_2$ exposure.

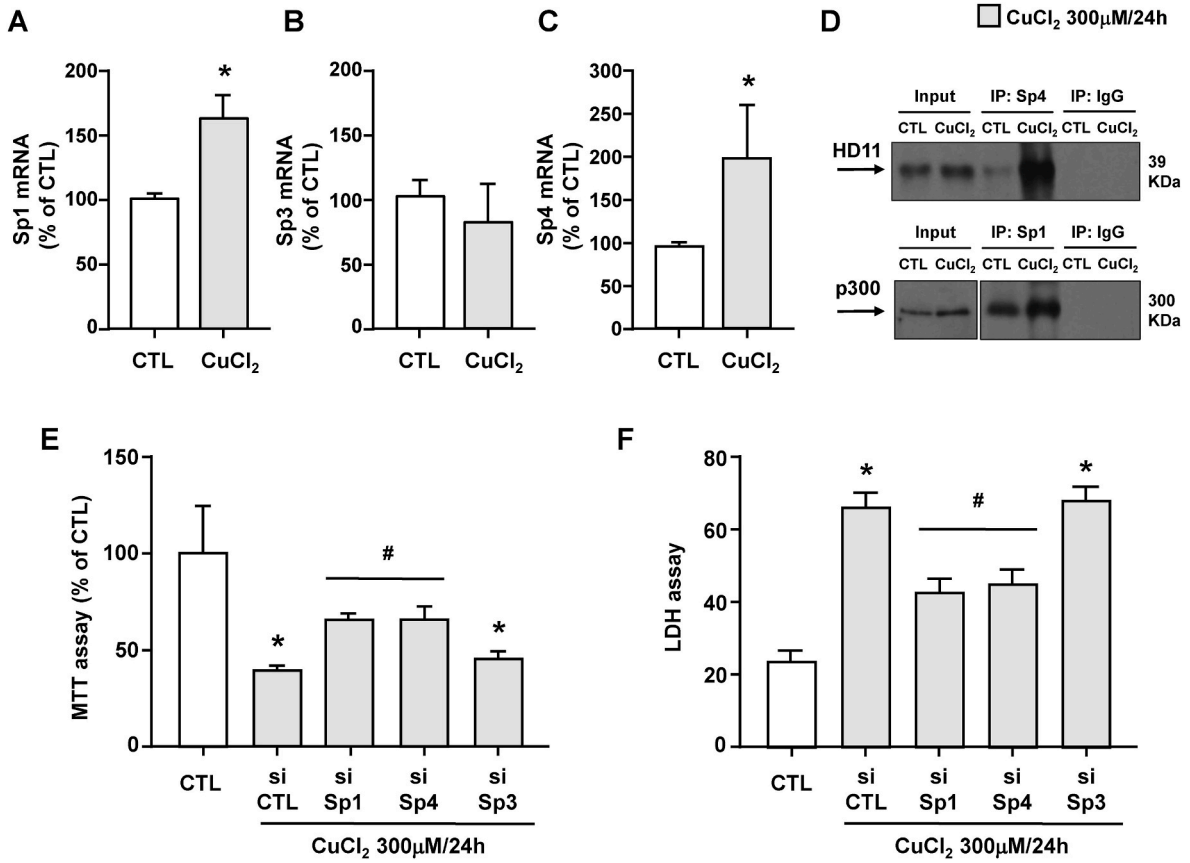

Fig. 2. Sp4 and Sp1, by interacting with HD11 and HAT-p300, respectively, were involved in $CuCl_2$-induced toxicity in SH-SY5Y cells. (**A-C**) RT-PCR for Sp1, Sp3, and Sp4 in cells exposed for 24 h to $CuCl_2$ (300 μM). Each bar represents mean ± SD obtained from 3 independent experimental sessions. *P < 0.05 vs CTL. (**D**) Representative Western blot showing immunoprecipitation between Sp4 and HD11 (upper panel) and between Sp1 and p300 (lower panel) in protein extracts from cells in control conditions (CTL) or after $CuCl_2$ exposure. (**E, F**) Effect of 300 μM $CuCl_2$ at 24 h, alone or after transfection of siRNAs against Sp1, Sp4 and Sp3, on mitochondrial activity (**E**) and LDH release (**F**). Each bar represents mean ± SD obtained from 4/5 independent experimental sessions. *P < 0.05 vs CTL; #P < 0.05 vs $CuCl_2$+ siCTL.

Interestingly, immunoprecipitation experiments showed that Sp1 bound with HAT-p300 (Fig. 2D, lower panel), but not with HD11 (data not shown), whereas Sp4 interacted with HD11 (Fig. 2D, upper panel), but not with HAT-p300 (data not shown). MTT and LDH experiments demonstrated that $CuCl_2$-dependent cell death was significantly reduced by transfection of siRNA against Sp1 and Sp4, but not by siRNA for Sp3 (Fig. 2E and F). Given that in SH-SY5Y cells $CuCl_2$-induced apoptosis occur via the increase of the pro-apoptotic gene BAX and the decrease of anti-apoptotic gene BCL-W (Xiang et al., 2021), we studied the effect of Sp1, Sp4, p300 and HD11 knocking-down on the mRNA and protein levels of BCL-W and BAX. As shown in Fig. 3A and B, the effect of $CuCl_2$ to induce BCL-W down-regulation was blocked by siSp4 and siHD11, but not by siSp1 and siHAT-p300. By contrast, Sp1 and HAT-p300 silencing counteracted the effect of $CuCl_2$ to increase BAX mRNA and protein, while siSp4 and siHD11 had no effect (Fig. 3C and D). These results indicated that in $CuCl_2$-treated cells, Sp4 and HD11 reduced the expression of BCL-W, whereas Sp1 and HAT-p300 up-regulated BAX.

2.3. $CuCl_2$ via Sp4 induced HD11 binding and hypoacetylation of histone H3 within BCL-W promoter sequence, and via Sp1 caused HAT-p300 binding and hyperacetylation of histone H4 within BAX promoter sequence in SH-SY5Y cells

We investigated in cells exposed to $CuCl_2$ the involvement of: (1) HD11 in Sp4-induced BCL-W reduction and (2) HAT-p300 in Sp1-induced BAX increase. As shown by ChIP analysis, HD11 binding to the BCL-W promoter increased after 24 h of treatment with $CuCl_2$; however, this binding resolved following transfection with siSp4, siHD11 and pre-treatment with the class IV HD inhibitor MOCE (Fig. 4A). Notably, siSp4 and siHD11 transfection or MOCE pre-treatment in cells exposed to $CuCl_2$, were able to revert the deacetylation of histone H3, but not of histone H4, within the BCL-W promoter (Fig. 4B and C). On the other hand, siSp1 and siHAT-p300 or the HAT-p300 inhibitor C646 were all able to counteract: (1) the increased binding of HAT-p300 (Fig. 4D) and (2) the consequent hyperacetylation of the histone H4 on the BAX gene promoter sequence (Fig. 4E), while they did not modulate histone H3 acetylation (Fig. 4F). These results suggested that Sp4 with HD11, and Sp1 with HAT-p300 formed two functional complexes on BCL-W and BAX promoter sequences, respectively, after $CuCl_2$ treatment.

2.4. Sp1/HAT-p300, by increasing the pro-apoptotic BAX, and Sp4/HD11, by reducing the anti-apoptotic BCL-W, are involved in copper-induced cell death in primary cortical neurons

To further validate our results, we investigated the role of Sp1/HAT-p300 and of Sp4/HD11 transcriptional complexes on the BAX and BCL-W genes in rat primary cortical neurons. Cells were exposed to different concentrations of $CuCl_2$ (1–1000 μM) for 24 h and a dose-related reduction in cell survival was observed (Fig. 5A). Notably, $CuCl_2$ at 100 μM was able to reduce cell viability by about 50 %, therefore this concentration was chosen for our further experiments. Interestingly, we found that 2 h pre-treatment with MOCE at 70 nM and C646 at 20 μM partially improved cell survival in cortical neurons exposed for 24 h

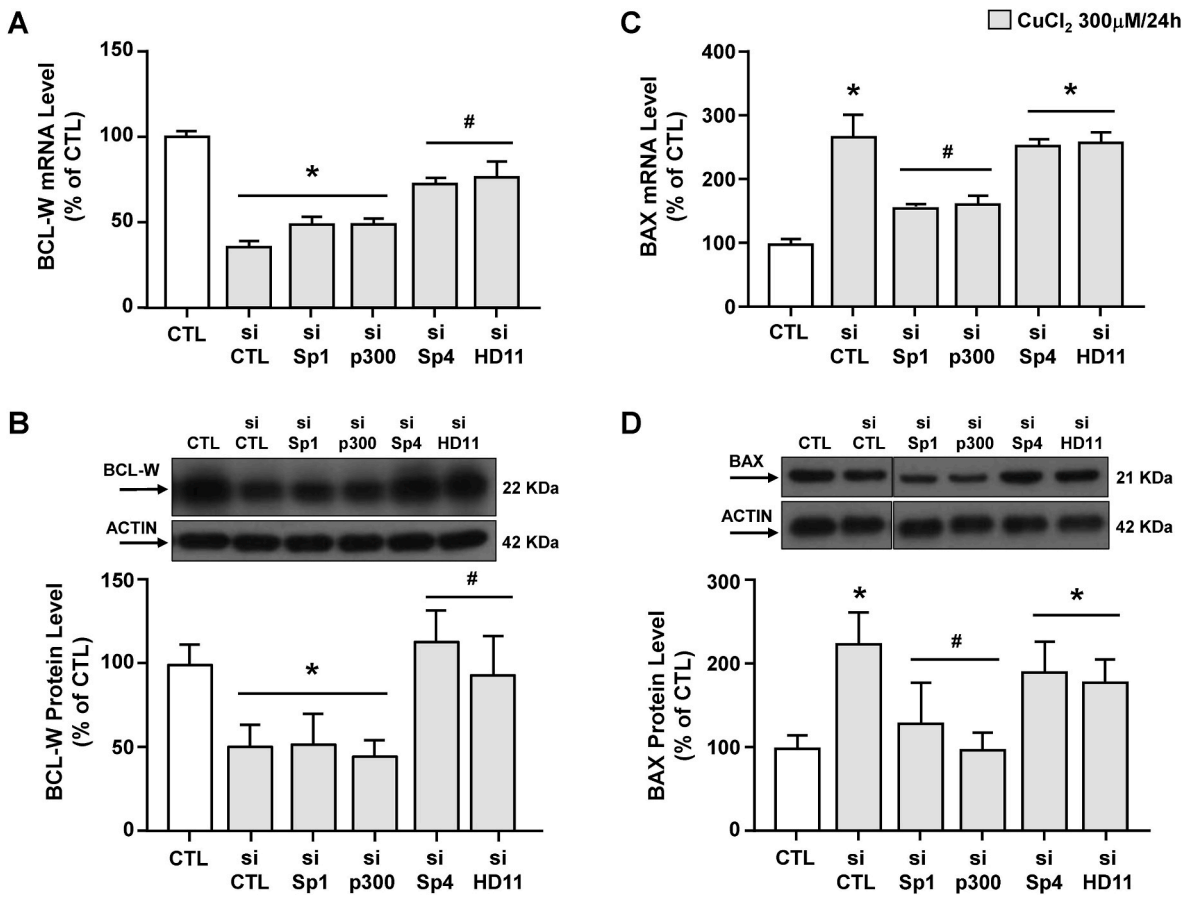

Fig. 3. Effect of Sp1, Sp4, HD11 and p300 knocking-down on $CuCl_2$-induced BCL-W down-regulation and BAX up-regulation in SH-SY5Y cells. (**A-D**) Effect of siRNAs against Sp1, Sp4, and Sp3 on BCL-W and BAX mRNA and protein expression levels, as revealed by RT-PCR and Western Blot analysis, in cells exposed for 24 h to $CuCl_2$ (300 μM). Each bar represents mean ± SD obtained from 3 to 4 independent experimental sessions. *P < 0.05 vs CTL. #P < 0.05 vs $CuCl_2$+ siCTL.

exposure to 100 μM $CuCl_2$. Noteworthy, the concomitant administration of MOCE and C646 completely prevented $CuCl_2$ neurotoxicity (Fig. 5B). As expected, the effect of $CuCl_2$ in increasing Sp1, HAT-p300, Sp4 and HD11 protein levels occurred after 12 and 24 h exposure (Fig. 5C–F). Moreover, the silencing by siRNAs transfection of Sp4 or HD11 were able to prevent $CuCl_2$-induced BCL-W mRNA down-regulation (Fig. 5 G), whereas the knocking-down of Sp1 or HAT-p300 blocked the effect of $CuCl_2$ in increasing BAX mRNA (Fig. 5 H). Lastly, MTT assay revealed a significant, but partial, increased survival following the single transfection of siRNAs against each TFs or epigenetic remodelers, while the combinations of siRNAs against Sp1/Sp4 and HD11/HAT-p300 completely prevented the $CuCl_2$-induced neurotoxicity (Fig. 5 I).

3. Materials and methods

3.1. Reagents

All common reagents were purchased from Sigma. Synthetic oligonucleotides were synthesized by Eurofins Genomic. The following siRNAs were used for human proteins: HDAC11 (siHD11) and p300 (sip300) (sc-106896, and sc-29431Santa Cruz Biotechnology), and Sp1 (siSp1), Sp4 (siSp4) (Guida et al., 2017). To silence rat proteins, we used siRNA for Sp1, Sp4 and p300 (Formisano et al., 2015) HDAC11 (sc-156104 Santa Cruz Biotechnology) and p300 (S102989693, Qiagen). For all the experiments, the siRNA CONTROL (siCTL) was from QIAGEN (All Stars Negative Control siRNA, cod: 1027280). Culture media and serum were purchased from Invitrogen. $CuCl_2$ powder (cod: 818247) was purchased from Sigma-Aldrich and dissolved in deionized water stock solution (10 mM). The stock solutions of ZVAD, MS-275, MC-1568, and C646 were already published and were used at non-toxic concentrations (Formisano et al., 2015; Guida et al., 2014; Laudati et al., 2019; von Coelln et al., 2001) Mocetinostat (MOCE) (sc-364539; Santa Cruz Biotechnology) stock solution (10 μM) and was used at 70 nM as already published (Huang et al., 2019). All drugs were diluted in cell culture medium; 0.1 % of dimethyl sulfoxide (DMSO) was the final concentration used as vehicle that did not cause cellular toxicity. Tali™ Apoptosis Kit-Annexin V Alexa Fluor™ 488 & Propidium Iodide was purchased from Invitrogen (cat: A10788).

3.2. Cell cultures

SH-SY5Y human neuroblastoma cells were cultured as previously reported (Laudati et al., 2019). $CuCl_2$ was diluted in culture medium at different final concentration (100 μM–500 μM in SH-SY5Y cells and 1 μM–1000 μM in rat cortical neurons). To reduce the change of responsiveness occurring in cells at high passage, all experiments were conducted in cultures containing cells between the 20th and 30th passages. The experiments on primary rat cortical neurons were performed following the experimental protocols approved by the Ethics Committee of "Federico II" University of Naples. Briefly, primary neurons were prepared from 17-day-old Sprague Dawley rat embryos (Charles River) and used after 9–11 days (DIV 9–11). We used 4 pregnant rats and 30 embryos overall. The pregnant Sprague Dawley rats (E17) were anesthetized following the ethical guidelines. A midline laparotomy was performed under sterile conditions to expose the uterus. The uterine horns were carefully removed and placed in cold Ca^{2+}/Mg^{2+}-free PBS with 30 mM glucose. Embryos were extracted, decapitated, and their brains were rapidly dissected under a stereomicroscope. The glial

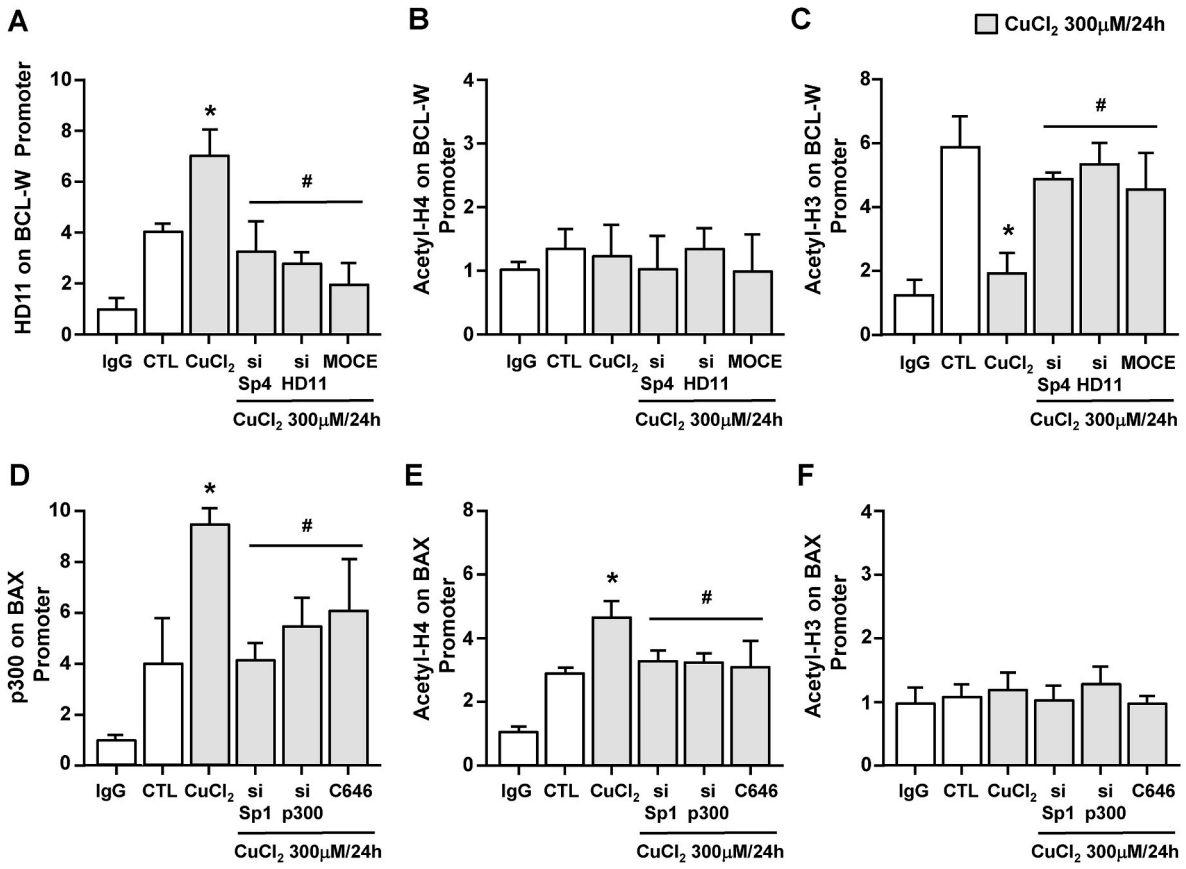

Fig. 4. siSp4, siHD11 or MOCE prevented the histone H3 hypoacetylation on BCL-W promoter whereas siSp1, sip300 or C646 counteracted the histone H4 hyperacetylation on BAX promoter in $CuCl_2$-treated SH-SY5Y cells. (**A-C**) Chromatin immunoprecipitation with: (**A**) anti-HD11, (**B**) anti-acetyl H4 histone (**C**) anti-acetyl H3 histone antibodies, followed by qPCR of BCLW promoter in cells exposed to $CuCl_2$ at 24 h, alone or with transfection of siRNAs against Sp4, HD11 or pre-treated with MOCE. (**D-F**) Chromatin immunoprecipitation with: (**D**) anti-p300, (**E**) anti-acetyl H4 histone (**F**) anti-acetyl H3 histone antibodies, followed by qPCR of BAX promoter in cells exposed to $CuCl_2$ at 24 h, alone or with transfection of siRNAs against Sp1, p300 or pre-treated with C646. IgG was used as negative control. The CTL group immunoprecipitated with IgG was defined as 1.0 and was used to compare the other experimental groups. Each bar represents mean ± SD obtained from 3 independent experimental sessions. *P < 0.05 vs CTL. #P < 0.05 vs $CuCl_2$.

inhibitor Cytosine Arabinoside (2.5 μM) was added at the second day of seeding to avoid glial contamination. The dissection was performed in $Ca^{2+/}Mg^{2+}$ free PBS containing glucose (30 mM). After 10 min of papain incubation at 37 °C, the tissues were treated in Earl's Balanced Salt Solution with DNase (0.16 U/ml), BSA (10 mg/ml), and ovomucoid (10 mg/ml) in order to separate them. The neurons were cultured in MEM/F12 with glucose, deactivated FBS (5 %), horse serum (5 %), glutamine (2 mm), penicillin (50 U/ml), and streptomycin (50 μg/ml) (Invitrogen). The neurons were then plated on plastic Petri dishes that were previously pre-coated with poly-D-lysine (20 μg/ml). The cellular density for: (1) MTT and LDH assays was of 1×10^6 cells/well in 24 well plates; (2) qRT-PCR was 5×10^6 cells/plate in 60 mm plates; (3) Western blot and ChIP was 15×10^6 cells/plate in 100 mm plates.

3.3. Drug treatment and siRNAs transfection

SH-SY5Y cells were pre-treated with anti-apoptotic inhibitor ZVAD (200 μM) for 2 h diluted in fresh medium (1 % FBS); regarding HDACs/HAT inhibitors, pre-treatment with MS-275 (1 μM), MC-1568 (1 μM), MOCE (70 nM) or C646 (20 μM) was carried for 2 h in complete medium (5 % FBS). After pre-treatments, cells were exposed to $CuCl_2$ (300 μM in SH-SY5Y or 100 μM in rat cortical neurons) for 24 h. SH-SY5Y cells and primary neurons were transfected with Lipofectamine 2000 (Thermo Fisher, cod: 11668027), following manufacturer's instructions. The efficiency of siRNAs transfection in SH-SY5Y cells was around 45 %, while the efficacy of the other siRNAs against siSp1, siSp4 was already reported in previous studies (Formisano et al., 2015).

3.4. MTT and LDH assay

MTT and LDH experiments were carried out as previously published in SH-SY5Y cells and cortical neurons (Laudati et al., 2019). After 24 h treatment with $CuCl_2$, alone or after pre-incubation with epi-drugs, MTT (0.5 mg/mL) was added to each well, and the cells were further incubated for 3 h at 37 °C with 5 % CO_2. Next, the supernatants were completely discharged and 100 μL of DMSO was added to each well to dissolve the formazan products. The amount of LDH released into the extracellular medium was quantified by using the Kit from Cayman (cod: E-BC-K771-M) and following the manufacturer's instructions. Cells treated with 1 % Triton X-100 were used as the positive control in LDH tests, and this value was indicative of 100 % cell death.

3.5. Cell death assay

To evaluate cell death, the Tali® Apoptosis kit - Annexin V Alexa Fluor® 488 and propidium iodide (Invitrogen) were used according to manufacturer's instructions (Chen et al., 2010). Cells after 24 h incubation with $CuCl_2$ were washed twice with PBS, trypsinized, resuspended in complete medium and analyzed using the apoptosis assay kit. Apoptotic cells showed green fluorescence, dead were yellow whereas live cells showed no fluorescence. For the analysis, cells were resuspended in 1000 μl of annexin binding and further 5 ml of Annexin V

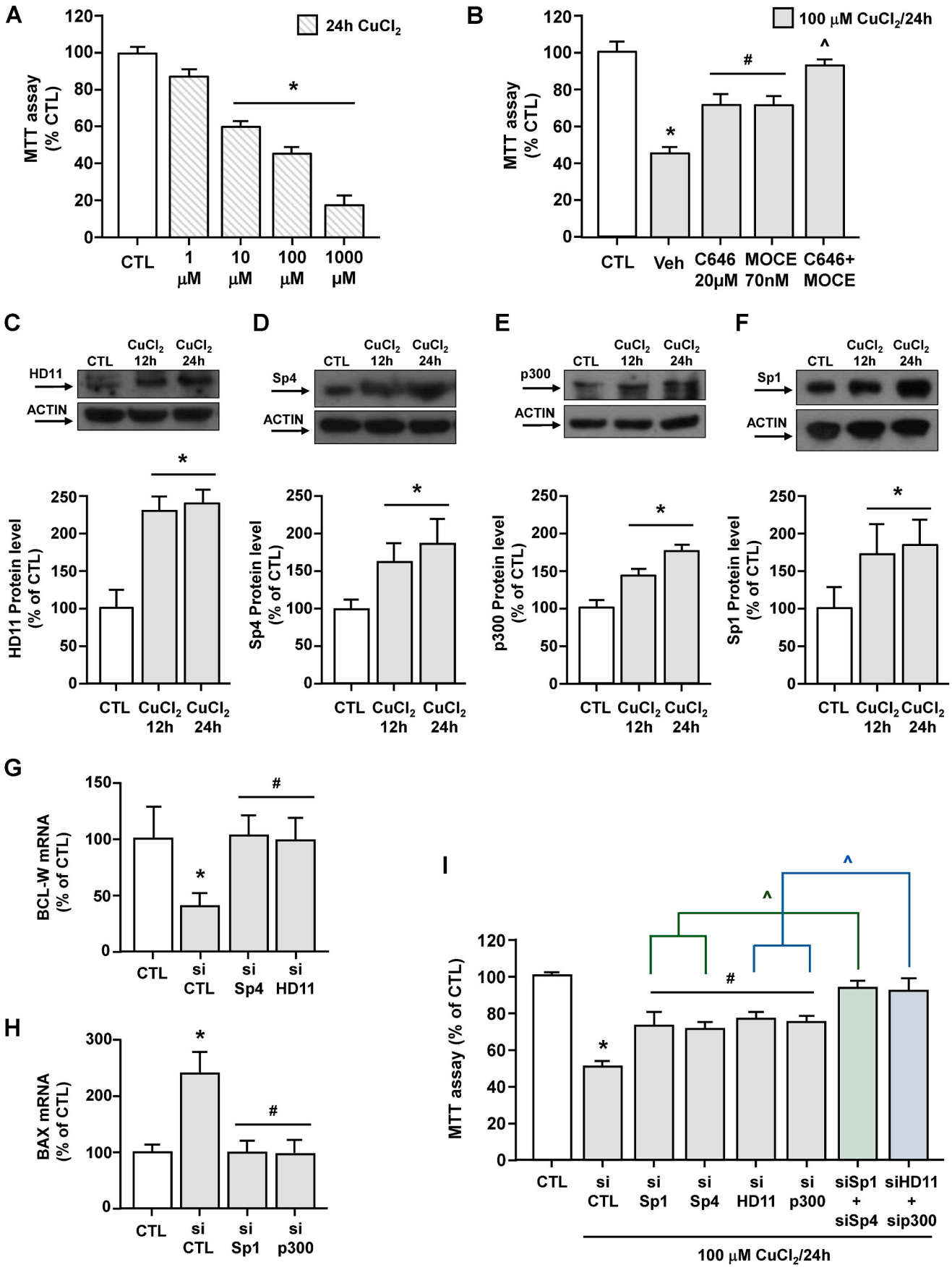

(caption on next page)

Fig. 5. Effect of siRNAs against Sp1, Sp4, HD11 and HAT-p300 in preventing CuCl2-induced cell death in rat cortical neurons. **(A)** Effects of 24 h exposure to CuCl2 at 1–1000 μM on cell death, as evaluated by MTT assay. Each bar represents mean ± SD obtained from 5 independent experimental sessions. *P < 0.05 vs CTL **(B)** MTT assay showing the effect of MOCE (70 nM) and C646 (1 μM), singly or in combination, in neurons exposed to CuCl2 at 24 h. Each bar represents mean ± SD obtained from 5 independent experimental sessions. *P < 0.05 vs CTL; #P < 0.05 vs CuCl2 + Vehicle. **(C–F)** Representative Western blot of HD11, Sp4, p300, and Sp1 in neurons treated for 12 and 24 h with CuCl2 (100 μM). Each bar represents mean ± SD obtained from 3 independentexperimental sessions. *P < 0.05 vs CTL. **(G, H)** Effect of siRNAs against: **(G)** Sp4 and HD11 on CuCl2 induced BCL-W mRNA reduction and **(H)** Sp1, and p300 on CuCl2-induced BAX mRNA up-regulation. Each bar represents mean ± SD obtained from 3 independent experimental sessions. *P < 0.05 vs CTL. #P < 0.05 vs CuCl2 + siCTL. **(I)** Experiments showing the effect of siSp1 and siSp4, alone or in combination, and of siHD11 and sip300, alone or in combination, on the mitochondrial activity in CuCl2-treated neurons. Each bar represents mean ± SD obtained from 5 independent experimental sessions. *P < 0.05 vs CTL. #P < 0.05 vs CuCl2 + siCTL. ∧ P < 0.05 vs siSp1, siSp4, siHD11 and sip300 alone.

Alexa Fluor® 488 was added in a adark room for 15 miutes. After that. cells were centrifuged at 1000 rpm for 5 min, resuspended in 100 ml of ABB, and 1 ml of Tali™ PI was added, and incubated in the dark at room temperature for 10 min. Samples evaluated analyzed with the Tali® Image-Based cytometer and identified using a Tali® Image-Based Cytometer (Invitrogen) and viable, apoptotic and necrotic cells were expressed as the percentage in the population.

3.6. Western blot analysis and immunoprecipitation

Immunoprecipitation was performed as previously reported (Formisano et al., 2015). Briefly, cells were collected in cold Phosphate Buffered Saline (PBS; Sigma, Milan IT). The cell pellet was resuspended in a RIPA lysis buffer (sc-24948, Santa Cruz Biotechnology) with 1X protease inhibitor and incubated on ice for 30 min. The lysate was then centrifuged at 12,000 rpm for 30 min at 4 °C to obtain proteins, for which Protein Assay (Bradford Reagent, Biorad, #5000006) was used to quantify protein extracts concentration. Then, 800 μg of protein was immunoprecipitated overnight at 4 °C using 3 μg of the following antibodies: (1) Anti-Sp4 (sc-645, Santa Cruz Biotechnology); (2) Anti-Sp1 (cat. No. GTX01528, GeneTex); (3) Normal Anti-Rabbit IgG antibody (Cat. No. GTX213110-01, GeneTex) as a negative control. The following day, the immune complexes were precipitated by adding 30 μl of Protein A/G PLUS-Agarose beads (sc-2003, Santa Cruz Biotechnology). The immune-precipitates were then subjected to Western blot analysis for HDAC11 and p300. Western blot analysis was performed as described elsewhere (Formisano et al., 2015). Proteins were separated on polyacrylamide gels and transferred onto nitrocellulose membranes (Nitrocellulose Transfer Packs, Biorad, #1704158) using the Semi-Dry TransBlot® System. Membranes were first blocked with EveryBlot Blocking Buffer (Cat. 12010020, Bio-Rad) and then incubated overnight at 4 °C in the blocking buffer with the following antibodies: Anti-HDAC11 (PA5-11249, Invitrogen, 1:1000), Anti-p300 (Cat. No. GTX30618, GeneTex, 1:1000), Anti-BAX (Cat. No. GTX10968, GeneTex, 1:500) Anti-BCL-W (SC-509 Santa Cruz Biotechnology, 1:1000) Anti-Sp1 (cat. No. GTX01528, GeneTex, 1:1000) Anti-Sp4 (sc-645, Santa Cruz Biotechnology, 1:500). After incubation with primary antibodies, membranes were washed with 0.1 % Tween 20 and then incubated with secondary antibodies for 1 h at room temperature. The analysis and quantification have been performed as already reported (G Laudati et al., 2019).

3.7. qRT-PCR

Trizol Reagent (Sigma, cod: T9424) was used to extract total RNA from cells in accordance with the vendor's instruction. Using the chemicals included in the Applied Biosystems™ High-Capacity cDNA Reverse Transcription Kit (Thermo Fisher Scientific, cod: 4368814), retrotranscription was performed on 2 μg of RNA in conformity with the manufacturer's directions and protocol (10 min at 25 °C, 2 h at 42 °C, 5 min at 85 °C, ∞ 4 °C). The obtained cDNA samples were amplified in triplicate by RT-qPCR with SYBR Green Real-Time PCR Master Mix (Thermo Fisher, cod: 4309155) as it follows: heating 2 min at 50 °C, denaturation 10 min at 95 °C, amplification and quantification 40 cycles of 30 s at 60 °C, with a single fluorescence measurement. qRT-PCR data were collected by using ABI Prism 7000 SDS software (Applied Biosystems).The expression of the genes of our interest was normalized to the expression of the housekeeping gene encoding for L-19(Guida et al., 2014) for human genes and HPRT (Formisano et al., 2015) for rat genes. Variations in mRNA levels were displayed as the mean of the relative quantification (RQ) values, that was determined as the threshold cycle difference (ΔCt) between the reference and target genes ($2^{-\Delta Ct} = RQ$). Regarding human genes, the primers used are the following: HDAC11 (Zhong et al., 2024); p300 FW: 5′ CCCCAGGGATGGGTTCTG 3′ p300 RV: 5′ CTGGATGAGTTTGCGCTTCTC 3'; Sp1 FW: 5′ TTGAAAAAGGAGTTGGTGGC 3′ Sp1 RV: 5′ TGCTGGTTCTGTAAGTTGGG 3; Sp3 FW: 5′ CCAGGATGTGGTAAAGTCTA3′ Sp3 RV: 5′ CTCCATTGTCTCATTTCCAG 3'; Sp4 FW: 5′ CTGACCAACTCAGACAAGTGCAT 3′ Sp4 RV: 5′ GGA CAC GAG CAG GCA ACT CT 3'; BAX FW: 5′ACATGGAGCTGCAGAGGATGA 3′ BAX RV: 5′ TGAAGTTGCCGTCAGAAAACA 3′ BCL-W FW: 5′ GAGGATTGTGGCCTTCTTTGAGT 3′ BCL-W RV: 5′ AGTCATCCACAGGGCGATGT3'. For rat genes, the primers used are the following: BAX FW: 5′ GCAGACGGCAACTTCAACTG 3′ BAX RV: 5′ TGATCAGCTCGGGCACTTTA 3′ and BCL-W FW: 5′ CCAGCATGCGACCTCTGTTT 3′ BCL-W RV: 5′ CCCAGGTATGCACCCAGAGT 3'

3.8. Chromatin immunoprecipitation (ChIP) assay

Cells were cross-linked with 1 % formaldehyde and then glycine (0.125 M), washed three times in cold PBS containing proteinase inhibitors and then collected in a buffer made of 50 mM Tris, pH 8.1, 1 % SDS, 10 mM EDTA, and anti-protease mixture. Chromatin was then fragmented by sonication (6 rounds of 10 s pulses at 50 % of potency) into 200–500 bp fragments, using Bandelin Sonopuls HD 2070 ultrasonic homogenizer (Bandelin). 50 μg of chromatin lysates were incubated overnight with 5 μg of the following antibody: p300 (Cat. No. GTX30618, GeneTex, 1:200), HDAC11 (PA5-11249, Invitrogen, 1:500), acetyl-histone H4 (Cat. No 06–866; 1:500 Sigma-Aldrich); acetyl-histone H3 (Cat. No 06–599; 1:500 Sigma-Aldrich), normal rabbit or mouse IgG were used as negative control. After immunoprecipitation, the DNA-histone complex was collected with 40 μl of Protein A/G PLUS-Agarose beads. After rotating for 2 h at 4 °C on a spinning wheel, the beads were washed with: (1) high-salt buffer (0.1 % SDS, 1 % Triton X-100, 2 mM EDTA, 20 mM Tris HCl pH 8.1, 500 mM NaCl); (2) low-salt buffer (0.1 % SDS, 1 % Triton X-100, 2 mM EDTA, 20 mM Tris HCl pH 8.1, 150 mM NaCl); (3) LiCl buffer (0.25 M LiCl, 1 % NP40, 1 % deoxycholate, 1 mM EDTA, 10 mM Tris HCl pH 8.1). TE buffer (10 mM Tris pH 8.1 and 1 mM EDTA) was used twice for the washing step held at room temperature. The precipitated fragments were eluted with a buffer containing 1 % SDS and 0.1 M NaHCO3. Amplification and quantification were performed as previously reported (Laudati et al., 2019) and the results obtained were normalized for the DNA input. The oligonucleotides used for the amplification of immunoprecipitated DNA were already published (Chen et al., 2010).

3.9. Statistical analysis

Data were analyzed by GraphPad Prism 5 software (Graph Pad Software, Inc.). All bars in the figures represent the mean ± S.D. Statistical differences between two experimental groups were analyzed

with the Student t-test. Statistically significant differences between more than two experimental groups were evaluated by one-way ANOVA, followed by Turkey's multiple comparison test. The number of independent experimental replicates were indicated in each figure legend.

4. Discussion

The results of the present study showed that $CuCl_2$ exposure increased the expression of the epigenetic complexes Sp4/HD11 and Sp1/HAT-p300 causing apoptotic death in neurons. Indeed, the activation of Sp4/HD11 reduced the expression of the anti-apoptotic gene BCL-W, whereas Sp1/HAT-p300 caused an increase of the pro-apoptotic gene BAX. Notably, preventing the formation of these two complexes completely counteracted $CuCl_2$-induced apoptotic neuronal death. These results are in accordance with Quiang et al. demonstrating that copper induces apoptosis: (1) in hippocampal neurons by reducing the expression of Bcl-2, and enhancing Bax (Lu et al., 2022b), (2) in SH-SY5Y by release of cytochrome *c* from mitochondria, and caspase-3 activation (Hirashima et al., 2010). At pharmacological level, we demonstrated that $CuCl_2$ neurotoxicity is partially prevented by the class IV HDs inhibitor MOCE, and by the HAT-p300 inhibitor C646, thus suggesting the involvement of the epigenetic eraser HD11 and epigenetic writer HAT-p300 in $CuCl_2$-reduced neuronal survival. Indeed, we found that siRNAs against HD11 and HAT-p300 reduced $CuCl_2$-induced cell death, both in SH-SY5Y cells and in cortical neurons. Furthermore, apoptotic cell death was the mechanism by which HD11 and HAT-p300 mediated cell death, indeed, MOCE and C646 are both able to reduce $CuCl_2$-induced increase in Annexin V staining, a known marker of apoptosis. These results are in accordance with the well-documented role of MOCE and C646 in reducing cell death. Specifically, MOCE exerts significant neuroprotection against the Aβ toxicity in primary neuronal cultures (Huang et al., 2019) and improved stroke-induced motor deficits (Kannangara and Vani, 2017), whereas C646 reduces apoptosis in prostate cell line by blocking HAT-p300 up regulation and (Santer et al., 2011) and in SH-SY5Y cells after sevoflurane exposure (Chen et al., 2021). Another interesting result is that $CuCl_2$ exposure caused an interaction between HD11 and Sp4 and between HAT-p300 and Sp1, and that these two specific epigenetic complexes are involved in $CuCl_2$ neurotoxicity. Notably, that Sp1 binds HAT-p300 has already been reported; indeed, Sp1 and HAT-p300 perform cooperative work in the transcriptional regulation of several genes (Lee and Workman, 2007), such as 12(S)-lipoxygenase (Hung et al., 2006) and p21 (Xiao et al., 2000), instead this is the first evidence showing that the transcription factor Sp4 binds to HD11. Furthermore, we found that transfection of siRNAs for Sp1 and Sp4 in cortical neurons ensured a reduction in $CuCl_2$-induced neuronal death, indicating that these two transcription factors are neurotoxic. Accordingly, Sp1 reduction is neuroprotective in cellular and mouse models of Huntington Disease (Qiu et al., 2006); whereas the overexpression of Sp4 caused neuronal death in MeHg-treated cells (Guida et al., 2017). Another relevant aspect of this paper is the characterization of a possible mechanism through which the Sp4/HD11 and Sp1/HAT-p300 protein complexes induce apoptosis in neuronal cells after exposure to $CuCl_2$. Specifically, we found in cells treated with $CuCl_2$: (1) a significant increase of the pro-apoptotic BAX gene and protein expression, that was counteracted by Sp1 or HAT-p300 knocking-down, and by C646 treatment, but not by siRNAs for Sp4 or HD11 and MOCE treatment; and (2) a strong reduction of the anti-apoptotic BCL-W mRNA and protein levels, that was prevented by Sp4 or HD11 knocking-down, and MOCE treatment, but not by siRNAs for Sp1 or HAT-p300 and C646 treatment. It is well documented that Sp1 and Sp4 can act as activators or repressors (Guida et al., 2017). In the present study it has been demonstrated that Sp1 is a transcriptional factor activating BAX, as already reported by others; indeed, neuronal oxidative stress induce cell apoptosis by increasing Sp1 binding on BAX gene promoter sequence (Deniaud et al., 2006). By contrast, that Sp4 isoform is a transcriptional repressor of BCL-W in neurons is apparently a new evidence, while it is known to repress neuronal genes, such as neurotrophin-3 (Ramos et al., 2009). Our results are in accordance with previous studies demonstrating the specificity of: (1) C646 to modulate the acetylation status of H4 histone tails (Dancy et al., 2012); (2) MOCE to induce H3 histone hyperacetylation via HD11; in fact, HD11 restricts hepatitis B virus (HBV) replication by inducing H3-, but not H4-deacetylation (Yuan et al., 2019). These results prompted us to hypothesize that the HD11 inhibitor MOCE partially reduces $CuCl_2$-induced cell death by preventing H3 histone deacetylation on the neuroprotective gene BCL-W, whereas the HAT-p300 inhibitor reduces $CuCl_2$-induced neurotoxicity by blocking H4 histone hyper-acetylation on the neurotoxic gene BAX. The results obtained in SH-SY5Y cells have been confirmed in cortical neurons, where we demonstrated that the effect of $CuCl_2$ to induce apoptosis occurs through: (1) the transcriptional activation of BAX via Sp1/HAT-p300 complex and (2) the transcriptional repression of BCL-W through Sp4/HD11 complex. Furthermore, since Sp1, Sp4, HD11 and HAT-p300 silencing partially counteracted $CuCl_2$-induced cell death, whereas the double knocking-down of Sp1 and Sp4 and of HD11 and HAT-p300 were effective in completely preventing $CuCl_2$-induced apoptosis, it could be hypothesized that the ratio between BAX/BCL-W is a critical step in commissioning apoptosis. Indeed, in our experimental conditions we found a concomitant BAX increase and BCL-W decrease, and treatment with siRNAs for Sp1 and HAT-p300 and C646 limited the up-regulation of BAX, but have any effect on BCL-W reduction. On contrary, siRNAs for Sp4, HD11 and MOCE counteracted $CuCl_2$-induced BCL-W reduction, but not BAX increase. These results indicate that only when equilibrium of the ratio between pro-apoptotic (represented by BAX) and anti-apoptotic (represented by BCL-W) genes is completely restored there is an effective inhibition of apoptosis. A limitation of the current study is that the experiments were conducted primarily using immortalized neuronal cell line such as SH-SY5Y and primary cortical neurons. These cell types may not fully replicate the complex interactions that occur in the brain, where different cell types, such as glial cells and endothelial cells, play critical roles in the response to copper toxicity. Future studies should be performed also *in vivo* to evaluate the activation of the identified pathway. In conclusion, our findings suggest that $CuCl_2$ induces apoptotic cell death by increasing BAX and reducing BCL-W expressions in neuronal cells; specifically, this effect is determined by the binding of Sp1/HAT-p300 and of Sp4/HD11 transcriptional complexes on BAX and BCL-W promoters, respectively, thereby making HDs/HATs possible new molecular targets in the pathogenesis of brain disorders linked to Copper overload. Furthermore, these results highlight the potential for targeting the Sp4/HD11 and Sp1/HAT-p300 complexes as therapeutic strategies for neurodegenerative diseases associated with copper dysregulation. Given the involvement of copper in neurodegeneration, the results could have broader implications for neurological diseases where copper homeostasis is disrupted such as Alzheimer's, Amyotrophic Lateral Sclerosis and Huntington's diseases.

CRediT authorship contribution statement

Silvia Ruggiero: Formal analysis, Data curation. **Natascia Guida:** Project administration, Methodology, Formal analysis, Data curation. **Luigi Mascolo:** Formal analysis, Data curation. **Angelo Serani:** Software, Formal analysis. **Anna Ferrante:** Formal analysis. **Francesca Galasso:** Formal analysis. **Luca Sanguigno:** Formal analysis, Data curation. **Erica Piemonte:** Methodology, Formal analysis, Data curation. **Elvira De Rosa:** Formal analysis, Conceptualization. **Paolo Montuori:** Writing – original draft, Supervision. **Maria Triassi:** Writing – original draft. **Gianfranco Di Renzo:** Writing – original draft. **Mario Galgani:** Writing – original draft, Conceptualization. **Luigi Formisano:** Writing – original draft, Supervision, Investigation.

Data availability

All data included in this study were available upon request by contacting the corresponding author.

Declaration of competing interest

The authors declare that they have no known competing financial interests or personal relationships that could have appeared to influence the work reported in this paper.

Acknowledgments

This work was supported by the following grant: MNESYS 2023 (PE0000006) by MIUR and National Recovery and Resilience Plan (NRRP) to Luigi Formisano.

Data availability

Data will be made available on request.

References

Arciello, M., Rotilio, G., Rossi, L., 2005. Copper-dependent toxicity in SH-SY5Y neuroblastoma cells involves mitochondrial damage. Biochem. Biophys. Res. Commun. 327, 454–459.

Broday, L., Peng, W., Kuo, M.H., Salnikow, K., Zoroddu, M., Costa, M., 2000. Nickel compounds are novel inhibitors of histone H4 acetylation. Cancer Res. 60, 238–241.

Chan, H.W., Liu, T., Verdile, G., Bishop, G., Haasl, R.J., Smith, M.A., Perry, G., Martins, R.N., Atwood, C.S., 2008. Copper induces apoptosis of neuroblastoma cells via post-translational regulation of the expression of Bcl-2-family proteins and the txJ mouse is a better model of hepatic than brain Cu toxicity. Int. J. Clin. Exp. Med. 1, 76.

Chen, A., Tan, B., Cheng, Y., 2021. P300 inhibition improves cell apoptosis and cognition impairment induced by sevoflurane through regulating IL-17a activation. World Neurosurg 154, e566–e571.

Chen, J., Wang, G., Wang, L., Kang, J., Wang, J., 2010. Curcumin p38-dependently enhances the anticancer activity of valproic acid in human leukemia cells. Eur. J. Pharmaceut. Sci. 41, 210–218.

Dancy, B.M., Crump, N.T., Peterson Daniel, J., Mukherjee, C., Bowers, E.M., Ahn, Young-Hoon, Yoshida, M., Zhang, J., Mahadevan, L.C., Meyers, D.J., Boeke, J.D., Cole, P.A., 2012. Live-cell studies of p300/CBP histone acetyltransferase activity and inhibition. Chembiochem 13, 2113–2121.

Deniaud, E., Baguet, J., Mathieu, A.-L., Pagès, G., Marvel, J., Leverrier, Y., 2006. Overexpression of Sp1 transcription factor induces apoptosis. Oncogene 25, 7096–7105.

Ejaz, H.W., Wang, W., Lang, M., 2020. Copper toxicity links to pathogenesis of Alzheimer's disease and therapeutics approaches. Int. J. Mol. Sci. 21, 1–33. https://doi.org/10.3390/IJMS21207660.

Enge, T.G., Ecroyd, H., Jolley, D.F., Yerbury, J.J., Kalmar, B., Dosseto, A., 2018. Assessment of metal concentrations in the SOD1G93A mouse model of amyotrophic lateral sclerosis and its potential role in muscular denervation, with particular focus on muscle tissue. Mol. Cell. Neurosci. 88, 319–329. https://doi.org/10.1016/J.MCN.2018.03.001.

Fitisemanu, F.M., Padilla-Benavides, T., 2024. Emerging perspectives of copper-mediated transcriptional regulation in mammalian cell development. Metallomics 16.

Formisano, L., Guida, N., Valsecchi, V., Cantile, M., Cuomo, O., Vinciguerra, A., Laudati, G., Pignataro, G., Sirabella, R., Di Renzo, G., Annunziato, L., 2015. Sp3/REST/HDAC1/HDAC2 complex represses and Sp1/HIF-1/p300 complex activates ncx1 gene transcription, in brain ischemia and in ischemic brain preconditioning, by epigenetic mechanism. J. Neurosci. 35, 7332–7348.

Gaetke, L.M., Chow-Johnson, H.S., Cho, C.K., 2014. Copper: toxicological relevance and mechanisms. Arch. Toxicol. 88, 1929–38.

Guida, N., Laudati, G., Anzilotti, S., Secondo, A., Montuori, P., Di Renzo, G., Formisano, 2015. Resveratrol via sirtuin-1 downregulates RE1-silencing transcription factor (REST) expression preventing PCB-95-induced neuronal cell death. Toxicol. Appl. Pharmacol. 288, 387–398.

Guida, N., Laudati, G., Galgani, M., Santopaolo, M., Montuori, P., Triassi, M., Di Renzo, G., Canzoniero, L.M., Formisano, L., 2014. Histone deacetylase 4 promotes ubiquitin-dependent proteasomal degradation of Sp3 in SH-SY5Y cells treated with di(2-ethylhexyl)phthalate (DEHP), determining neuronal death. Toxicol. Appl. Pharmacol. 280 (1), 190–8.

Guida, N., Laudati, G., Mascolo, L., Cuomo, O., Anzilotti, S., Sirabella, R., Santopaolo, M., Galgani, M., Montuori, P., Di Renzo, G., Canzoniero, L.M., Formisano, L., 2016. MC1568 inhibits thimerosal-induced apoptotic cell death by preventing HDAC4 up-regulation in neuronal cells and in rat prefrontal cortex. Toxicol. Sci. 154, 227–240.

Guida, N., Laudati, G., Mascolo, L., Valsecchi, V., Sirabella, R., Selleri, C., Di Renzo, G., Canzoniero, L.M., Formisano, L., 2017. p38/Sp1/Sp4/HDAC4/BDNF axis is a novel molecular pathway of the neurotoxic effect of the methylmercury. Front. Neurosci. 19, 11–8.

Hands, S.L., Mason, R., Sajjad, M.U., Giorgini, F., Wyttenbach, A., 2010. Metallothioneins and copper metabolism are candidate therapeutic targets in Huntington's disease. Biochem. Soc. Trans. 38, 552–558. https://doi.org/10.1042/BST0380552.

Hirashima, Y., Seshimo, S., Fujiki, Y., Okabe, M., Nishiyama, K., Matsumoto, M., Kanouchi, H., Oka, T., 2010. Homocysteine and copper induce cellular apoptosis via caspase activation and nuclear translocation of apoptosis-inducing factor in neuronal cell line SH-SY5Y. Neurosci. Res. 67, 300–306.

Huang, H.-J., Huang, H.-Y., Hsieh-Li, H.M., 2019. MGCD0103, a selective histone deacetylase inhibitor, coameliorates oligomeric Aβ25-35 -induced anxiety and cognitive deficits in a mouse model. CNS Neurosci. Ther. 25, 175–186.

Hung, J.J., Wang, Y.T., Chang, W.C., 2006. Sp1 deacetylation induced by phorbol ester recruits p300 to activate 12(S)-lipoxygenase gene transcription. Mol. Cell Biol. 26, 1770–1785.

Joshi, A., Farber, K., Scheiber, I.F., 2021. Neurotoxicity of copper and copper nanoparticles. Adv Neurotoxicol 5, 115–157. https://doi.org/10.1016/BS.ANT.2020.11.001.

Kalita, J., Kumar, V., Misra, U.K., Bora, H.K., 2017. Memory and learning dysfunction following copper toxicity: biochemical and immunohistochemical basis. Mol. Neurobiol. 55 (5), 3800–3811.

Kang, J., Lin, C., Chen, J., Liu, Q., 2004. Copper induces histone hypoacetylation through directly inhibiting histone acetyltransferase activity. Chem. Biol. Interact. 148, 115–123.

Kannangara, T.S., Vani, M.A., 2017. Delayed treatment with histone deacetylase inhibitors promotes stroke Recovery. J. Neurosci. 37, 12088–12090.

Kolbaum, A.E., Sarvan, I., Bakhiya, N., Spolders, M., Pieper, R., Schubert, J., Jung, C., Hackethal, C., Sieke, C., Grünewald, K.H., Lindtner, O., 2023. Long-term dietary exposure to copper in the population in Germany - results from the BfR MEAL study. Food Chem. Toxicol. 176. https://doi.org/10.1016/J.FCT.2023.113759.

Laudati, G., Mascolo, L., Guida, N., Sirabella, R., Pizzorusso, V., Bruzzaniti, S., Serani, A., Di Renzo, G., Canzoniero, L.M.T., Formisano, L., 2019. Resveratrol treatment reduces the vulnerability of SH-SY5Y cells and cortical neurons overexpressing SOD1-G93A to Thimerosal toxicity through SIRT1/DREAM/PDYN pathway. Neurotoxicology 71, 6–15.

Lee, K.K., Workman, J.L., 2007. Histone acetyltransferase complexes: one size doesn't fit all. Nat. Rev. Mol. Cell Biol. 8, 284–295.

Liang, Z.D., Tsai, W.B., Lee, M.Y., Savaraj, N., Kuo, M.T., 2012. Specificity protein 1 (sp1) oscillation is involved in copper homeostasis maintenance by regulating human high-affinity copper transporter 1 expression. Mol. Pharmacol. 81, 455–464.

Lin, C., Kang, J., Zheng, R., 2005. Oxidative stress is involved in inhibition of copper on histone acetylation in cells. Chem. Biol. Interact. 151, 167–176.

Lomonosova, E., Chinnadurai, G., 2008. BH3-only proteins in apoptosis and beyond: an overview. Oncogene 27 (Suppl. 1), S2–S19.

Lu, Q., Zhang, Y., Zhao, C., Zhang, H., Pu, Y., Yin, L., 2022a. Copper induces oxidative stress and apoptosis of hippocampal neuron via pCREB/BDNF/and Nrf2/HO-1/NQO1 pathway. J. Appl. Toxicol. 42, 694–705.

Lu, Q., Zhang, Y., Zhao, C., Zhang, H., Pu, Y., Yin, L., 2022b. Copper induces oxidative stress and apoptosis of hippocampal neuron via pCREB/BDNF/and Nrf2/HO-1/NQO1 pathway. J. Appl. Toxicol. 42, 694–705.

Min, S.-W., Cho, S.-H., Zhou, Y., Schroeder, S., Haroutunian, V., Seeley, W.W., Huang, E. J., Shen, Y., Masliah, E., Mukherjee, C., Meyers, D., Cole, P.A., Melanie, Ott, Gan, L., 2010. Acetylation of tau inhibits its degradation and contributes to tauopathy. Neuron 67, 953–966.

Pal, A., Badyal, R.K., Vasishta, R.K., Attri, S.V., Thapa, B.R., Prasad, R., 2013. Biochemical, histological, and memory impairment effects of chronic copper toxicity: a model for non-wilsonian brain copper toxicosis in Wistar rat. Biol. Trace Elem. Res. 153, 257–268. https://doi.org/10.1007/S12011-013-9665-0/FIGURES/17.

Qiu, Z., Norflus, F., Singh, B., Swindell, M.K., Buzescu, R., Bejarano, M., Chopra, R., Zucker, B., Benn, C.L., Dirocco, D.P., Cha, J.H., Ferrante, R.J., Hersch, S.M., 2006. Sp1 is up-regulated in cellular and transgenic models of Huntington disease, and its reduction is neuroprotective. J. Biol. Chem. 281, 16672–16680.

Ramos, B., Val\'\in, A., Sun, X., Gill, G., 2009. Sp4-dependent repression of neurotrophin-3 limits dendritic branching. Mol. Cell. Neurosci. 42, 152–159.

Rehman, M., Liu, L., Wang, Q., Saleem, M.H., Bashir, S., Ullah, S., Peng, D., 2019. Copper environmental toxicology, recent advances, and future outlook: a review. Environ. Sci. Pollut. Res. Int. 26, 18003–18016. https://doi.org/10.1007/S11356-019-05073-6.

Santer, F.R., Hoschele, P.P., Oh, S.J., Erb, H.H., Bouchal, J., Cavarretta, I.T., Parson, W., Meyers, D.J., Cole, P.A., 2011. Inhibition of the acetyltransferases p300 and CBP reveals a targetable function for p300 in the survival and invasion pathways of prostate cancer cell lines. Mol. Cancer Therapeut. 10, 1644–1655.

Seto, E., Yoshida, M., 2014. Erasers of histone acetylation: the histone deacetylase enzymes. Cold Spring Harbor Perspect. Biol. 6.

Sheline, C.T., Choi, E.H., Kim-Han, J.S., Dugan, L.L., Choi, D.W., 2002. Cofactors of mitochondrial enzymes attenuate copper-induced death in vitro and in vivo. Ann. Neurol. 52, 195–204.

Song, I.S., Chen, H.H., Aiba, I., Hossain, A., Liang, Z.D., Klomp, L.W., Kuo, M.T., 2008. Transcription factor Sp1 plays an important role in the regulation of copper homeostasis in mammalian cells. Mol. Pharmacol. 74, 705–713.

Song, M.O., Li, J., Freedman, J.H., 2009. Physiological and toxicological transcriptome changes in HepG2 cells exposed to copper. Physiol. Genom. 38, 386–401.

Squitti, R., Pasqualetti, P., Dal Forno, G., Moffa, F., Cassetta, E., Lupoi, D., Vernieri, F., Rossi, L., Baldassini, M., Rossini, P.M., 2005. Excess of serum copper not related to

ceruloplasmin in Alzheimer disease. Neurology 64, 1040–1046. https://doi.org/10.1212/01.WNL.0000154531.79362.23.
Squitti, R., Siotto, M., Polimanti, R., 2014. Low-copper diet as a preventive strategy for Alzheimer's disease. Neurobiol. Aging 35 (Suppl. 2). https://doi.org/10.1016/J.NEUROBIOLAGING.2014.02.031.
Sun, Y., Liu, C., Liu, Y., Hosokawa, T., Saito, T., Kurasaki, M., 2014. Changes in the expression of epigenetic factors during copper-induced apoptosis in PC12 cells. Journal of Environmental Science and Health, Part A 49, 1023–1028.
Tokuda, E., Okawa, E., Ono, S.I., 2009. Dysregulation of intracellular copper trafficking pathway in a mouse model of mutant copper/zinc superoxide dismutase-linked familial amyotrophic lateral sclerosis. J. Neurochem. 111, 181–191. https://doi.org/10.1111/J.1471-4159.2009.06310.X.
Tümer, Z., Møller, L.B., 2010. Menkes disease. Eur. J. Hum. Genet. 18, 511–518. https://doi.org/10.1038/EJHG.2009.187.
Vanlandingham, J.W., Tassabehji, N.M., Somers, R.C., Levenson, C.W., 2005. Expression profiling of p53-target genes in copper-mediated neuronal apoptosis. NeuroMolecular Med. 7, 311–324.
von Coelln, R., K'ugler, S., B'ahr, M., Weller, M., Dichgans, J., Schulz, J.B., 2001. Rescue from death but not from functional impairment: caspase inhibition protects dopaminergic cells against 6-hydroxydopamine-induced apoptosis but not against the loss of their terminals. J. Neurochem. 77, 263–273.
Wu, Z., Song, X., Wang, G., Wang, B., 2024. U-shaped nonlinear relationship between dietary copper intake and peripheral neuropathy. Sci. Rep. 14 (1 14), 1–8. https://doi.org/10.1038/s41598-024-76159-6, 2024.
Xiang, B., Li, D., Chen, Y., Li, M., Zhang, Y., Sun, T., Tang, S., 2021. Curcumin ameliorates copper-induced neurotoxicity through inhibiting oxidative stress and mitochondrial apoptosis in SH-SY5Y cells. Neurochem. Res. 46, 367–378.
Xiao, H., Hasegawa, T., Isobe, K.-I., 2000. P300 collaborates with Sp1 and Sp3 in p21/promoter activation induced by histone deacetylase inhibitor. J. Biol. Chem. 275, 1371–1376.
Yuan, Y., Zhao, K., Yao, Y., Liu, Canyu, Chen, Y., Li, J., Wang, Y., Pei, Rongjuan, Chen, J., Hu, X., Zhou, Y., Wu, Chunchen, Chen, X., 2019. HDAC11 restricts HBV replication through epigenetic repression of cccDNA transcription. Antivir. Res. 172, 104619.
Zhong, G., Wang, X., Li, J., Xie, Z., Wu, Q., Chen, J., Wang, Y., Chen, Z., Cao, X., Li, T., Liu, J., Wang, Q., 2024. Insights into the role of copper in neurodegenerative diseases and the therapeutic potential of natural compounds. Curr. Neuropharmacol. 22, 1650–1671.
Zubčić, K., Hof, P.R., Šimić, G., Jazvinšćak Jembrek, M., 2020. The role of copper in tau-related pathology in Alzheimer's disease. Front. Mol. Neurosci. 13. https://doi.org/10.3389/FNMOL.2020.572308.